Free Radical Biology and Medicine 189 (2022) 32–41

Contents lists available at ScienceDirect

Free Radical Biology and Medicine

journal homepage: www.elsevier.com/locate/freeradbiomed

Cold atmospheric plasma enhances doxorubicin selectivity in metastasic bone cancer

Miguel Mateu-Sanz [a,b,c], María-Pau Ginebra [a,b,c], Juan Tornín [a,b,c,d,e,**], Cristina Canal [a,b,c,*]

[a] Biomaterials, Biomechanics and Tissue Engineering Group, Materials Science and Engineering Department, and Research Center for Biomedical Engineering, Universitat Politècnica de Catalunya (UPC), Escola d'Enginyeria Barcelona Est (EEBE), c/Eduard Maristany 14, 08019, Barcelona, Spain
[b] Barcelona Research Center in Multiscale Science and Engineering, UPC, 08019, Barcelona, Spain
[c] Institut de Recerca Sant Joan de Déu, 08034, Barcelona, Spain
[d] Sarcomas and Experimental Therapeutics Laboratory, Instituto de Investigación Sanitaria del Principado de Asturias (ISPA), Hospital Universitario Central de Asturias, Avenida de Roma, s/n, 33011, Oviedo, Spain
[e] Instituto Universitario de Oncología del Principado de Asturias, 33011, Oviedo, Spain

ARTICLE INFO

Keywords:
Cold Atmospheric Plasmas
Plasma Conditioned Liquids
Prostate Cancer
Bone Metastasis
Doxorubicin

ABSTRACT

High-dose systemic chemotherapy constitutes a main strategy in the management of bone metastases, employing drugs like doxorubicin (DOX), related with severe side effects. To solve this issue, Cold Atmospheric Plasmas (CAP) have been proposed as potential non-invasive anti-cancer agents capable of improving the efficacy of traditional drugs. Here, we investigate the cytotoxic effects of Plasma Conditioned Medium (PCM) in combination with DOX in prostate cancer cells from bone metastases (PC-3) as well as in non-malignant bone-cells. PCM was able to enhance the cytotoxic potential of DOX both in monolayer and in a 3D bioengineered model mimicking the bone matrix. The combined treatment of PCM + DOX resulted in a profound downregulation of the redox defenses (*CAT1, SOD2, GPX1*) and drug resistance genes (*MRP1, MDR1, BCRP1*), resulting in an enhanced uptake of DOX coupled to an overload of intracellular ROS. Besides, PCM improved the cytotoxic potential of DOX interfering on the migratory and clonogenic potential of PC-3 cells. Importantly, non-malignant bone cells were unaffected by the combination of PCM + DOX. Overall, these new findings may represent a new therapeutic approach for the management of bone metastatic prostate cancer in the future.

1. Introduction

Primary tumors like breast, prostate, lung, gastrointestinal and thyroid among others usually metastasize to bone, aggravating the prognosis of these patients [1]. Overall, despite the implementation and continuous optimization of multimodal therapies, survival data of bone metastatic patients remains fatal. The usual management of bone metastases associates surgery - when it is possible - and systemic delivery of standard chemotherapeutics when tumors are advanced or unresectable, employing drugs like cisplatin or doxorubicin (DOX) [2]. Unfortunately, in this kind of tumors, the bone environment acts as a barrier for drug diffusion [3] and it is necessary to apply high systemic doses to obtain appropriate activity [2]. Notably, these high doses of systemic drugs are associated with negative side effects. For example, DOX induces complications in non-targeted tissues; the literature shows that cardiotoxicity is a main sequel of DOX, but it also affects other organs like the brain, kidney and liver [4]. For these reasons, new strategies aiming to improve the anti-tumor activity of conventional drugs and allow to reduce their dose are urgently required.

In the search for novel therapeutic options, Cold Atmospheric Plasmas (CAP) have come to the limelight. In physics, plasma is known as the fourth state of matter and can be artificially produced when a gas is subjected to an electrical discharge. This excited state includes ultraviolet (UV) and visible light, electromagnetic fields, photons, electrons, ions and a wide range of Reactive Oxygen and Nitrogen Species (RONS). CAP operate at atmospheric pressure and body temperatures,

Abbreviations: DOX, Doxorubicin; PCL, Plasma Conditioned Liquids; CAP, Cold Atmospheric Plasma; PCM, Plasma Conditioned Medium.

* Corresponding author. Biomaterials, Biomechanics and Tissue Engineering Group, Dpt. Materials Science and Engineering and Research Center for Biomedical Engineering, Technical University of Catalonia (UPC), Escola d'Enginyeria Barcelona Est (EEBE), c/ Eduard Maristany 14, 08019, Barcelona, Spain.
** Corresponding author. Sarcomas and Experimental Therapeutics Laboratory, Instituto de Investigación Sanitaria del Principado de Asturias (ISPA), Hospital Universitario Central de Asturias, Avenida de Roma, s/n, 33011, Oviedo, Spain.
E-mail addresses: juantornin@ispasturias.es (J. Tornín), cristina.canal@upc.edu (C. Canal).

https://doi.org/10.1016/j.freeradbiomed.2022.07.007
Received 10 May 2022; Received in revised form 20 June 2022; Accepted 11 July 2022
Available online 14 July 2022

allowing their application to living cells and tissues. Today, we can find a wide range of biomedical applications of CAP, such as pathogen decontamination [5,6], wound healing [7–9], blood coagulation [10] and interestingly, many researchers propose CAP as promising anti-cancer approach [11].

Despite the promising results obtained by the application of CAP to treat superficial tumors [12,13], their role against tumors located in inner regions of the body, like bone cancers, is limited due the presence of body barriers. For this reason, the ability to transfer RONS into a carrier liquid as a result of CAP treatment is of particular interest [14,15]. These CAP-treated liquids have been described in the literature as Plasma Conditioned Liquids (PCL). When cell culture medium is the target liquid it is designated as Plasma Conditioned Media (PCM) and has been widely employed, especially for *in vitro* research, as it has been shown that the effects observed are easily transposable to other PCL such as saline solutions of potential application in the clinics. PCL contain the long-lived RONS produced by CAP, such as H_2O_2, NO_2^- and NO_3^- among others. These RONS can be transferred to cancer cell cultures [16] or tumors [14,15] inducing cytotoxic effects.

In addition, several studies have shown that both CAP and PCL treatment can increase the effect of conventional drugs by different mechanisms in *in vitro* [17–22] and *in vivo* [23,24] studies. For example, both CAP and PCL in combination with cisplatin or DOX induced additive effects in several cancers like melanoma, glioblastoma and pancreatic cancer, by increasing drug uptake [22,25,26] and intracellular ROS induction [27,28]. Considering that both types of drugs act by binding to DNA and producing ROS [29], it is suggested that a summative effect of CAP or PCL may increase the effect on cancer cells and decrease the effective dose required of the chemotherapeutic agent [30].

Notably, most research related to CAP and PCL in the field of cancer has been done in monolayer cultures, obviating the importance of the 3D tissue micro-environment. As an alternative to 2D models, bioengineered tumor models open the door to the development of more advanced preclinical models, recreating the 3D tumor microenvironment to anticipate clinical responses [31,32]. Bioengineered models may be especially relevant in the management of bone cancers [33], where the bone micro-environment has a crucial role on drug resistance [34,35].

We recently demonstrated the efficiency of PCL against primary bone cancers, by inducing an increase of the intracellular ROS that triggers DNA damage and subsequent apoptosis [36,37]. Notably, we observed that PCL showed diminished cytotoxic potential in 3D engineered primary bone tumor compared with the treatment of 2D cultures by favoring the evasion from oxidative stress and selecting the PCL-resistant cell populations [38].

Our hypothesis is that the CAP-generated RONS in PCM can be used to foster the anti-cancer effect of DOX in bone metastatic prostate cancer. It is therefore our aim to investigate the potential of the combined effect of PCM and DOX on metastatic bone cancer in a relevant scenario. Thus, we developed a 3D engineered tumor model using a metastatic prostate cancer cell line (PC-3) to take into account the bone extracellular matrix, and we used kINPen ® IND, a cold-plasma jet approved in clinical trials, to produce PCM and apply it over PC-3, human Bone Marrow Mesenchymal Stem Cells (hBM-MSCs) and human osteoblasts (hOBs) to explore the selectivity and efficacy of the proposed approach.

2. Materials and methods

2.1. Cell culture

PC-3 cells were purchased from BioNova (REF EP-CL-0304) and were cultured in RPMI medium (GibcoTM, Carlsbad, CA, USA) supplemented with 10% of fetal bovine serum (FBS) and penicillin/streptomycin (50 U/mL and 50 μg/mL, respectively), all from GibcoTM. Passages 1–29 were used in all experiments. Human osteoblasts (hObs) were purchased from Sigma-Aldrich and were cultured in Osteoblast Growth Medium (PromoCell). Human bone marrow mesenchymal stem cells (hBM-MSCs) were purchased from ATCC and were cultured in advanced DMEM supplemented with 10% of fetal bovine serum (FBS) and penicillin/streptomycin (50 U/mL and 50 μg/mL, respectively), all from GibcoTM. They were expanded and cultured at 37 °C in a 95% humidified atmosphere containing 5% of CO_2. In both, passages 1–10 were used in all experiments.

2.2. CAP treatment and production of PCM

kINPen ® IND (Neoplas tools GmbH, Greifswald, Germany) was employed in this study, which is a commercial plasma jet tool that consists of a hand-held unit that discharges plasma under atmospheric conditions, employing a DC power unit and Argon gas to generate the plasma. In the centre of a ceramic capillary (inner diameter 1.6 mm) a pin-type electrode (1 mm diameter) is mounted, and a ring around the dielectric as grounded counter-electrode. The needle is powered by a small RF generator producing a sinusoidal voltage waveform ranging from 2 kV to 3 kV amplitude peak at a frequency of 1 MHz and modulated with 2.5 kHz and a plasma duty cycle of 1:1. Direct CAP was performed by treating cell cultures seeded in 24 well-plates and covered by 1 mL of fresh RPMI medium with kINPEN ® IND at a distance of 10 mm from the surface of the liquid during 15–120 s employing a z-positioner, while PCM was produced at same conditions without cells. Then, cell culture medium was removed and discarded from each well containing cells and replaced with 1 mL per well of PCM until analysis as described in Ref. [16].

2.3. Cell viability in monolayer

Cell viability assays were performed as descrived in Ref. [16]. Briefly, PC-3 were seeded at a density of 3 X 10^4 per well in 24 well-plates. 24 h after seeding, culture medium was replaced by PCM obtained by plasma treatment of cell culture medium during 15–120 s. Then, cells were incubated in contact with 1 mL this PCM until analysis. H_2O_2 and NO_2^- produced in PCM were quantified as described in Ref. [16]. Cell viability was evaluated 24 and 72 h after treatment. In addition, PC-3 were exposed to DOX concentrations of 0,01–100 μM (logaritmic doses) in RPMI or in PCM treated during 30 s added after CAP treatment and cell viability was evaluated after 24 h. Then, hBM-MSCs, hObs and PC-3 were exposed to PCM treated during 30 s, with DOX 10 μM and with combination of these, and cell viability were measured 24 and 72 h after treatment (n=4). In all cases, cell viability was evaluated by WST-1 assay at working solution of 18 μL/mL in RPMI.

2.4. DOX uptake and intracellular ROS

From this section on, we exposed cells to PCM obtained by 30 s plasma treatment, to DOX 10 μM and to combination of both for all the experiments. Intracellular levels of ROS were measured using 2′,7′-Dichlorofluorescin diacetate (DCFH-DA). For this, PC-3 were sedded in standard conditions and they were incubated before treatment with 40 μM of DCFH-DA in DPBS during 1 h, prepared from 2 mM of DCFH-DA solved in DMSO. Afterwards, cells were washed with DPBS and exposed to 1 mL of PCM treated in the previously described conditions. Fluorescence of DCFH-DA and of DOX were quantified at time 0 and after 30 min, 1 h, 2 h and 6 h of exposition to each treatment by replacing them with 500 μL of DPBS (n=3). The λex/em was of 490/530 nm for DCFH-DA and 530/590 nm for DOX.

2.5. DNA damage

PC-3 were treated as described in previous section (n=3) and after that, cells were fixed with PFA 4%, washed and blocked with 5% BSA in PBS-0.1% Tween-20 and incubated with mouse Anti-phospho-Histone γH2AX (Ser139) Antibody, clone JBW301 (Merk Millipore, Burlington,

MS, USA) at 4°C in agitation overnight. After that, primary antibody was washed and cells were incubated with secondary antibody Alexa Fluor 488 goat anti-mouse (Invitrogen) for 30 min in the dark. Then, cells were washed, and samples were mounted with ProLong™ Gold Antifade Mountant with DAPI (LifeTechnologies, Carlsbad, CA, USA). Images were captured using Zeiss laser scanning microscope. DNA damage were estimated by image analysis employing ImageJ as described in Ref. [37].

2.6. qRT-PCR

RNA of treated samples were isolated employing RNAeasy Mini Kit (Qiagen) following manufacturer's protocol (n=3). Then, cDNA synthesis was performed using the Maxima First Strand cDNA Synthesis Kit for qRT-PCR, with dsDNase (Thermo Scientific, #K1671), 1 μG mRNA was loaded. The gene expression was assessed by using QuantiNova Fast SYBR™ Green PCR Master Mix (Qiagen) and employing a Magnetic Induction Cycler (MIC) qPCR equipment (Bio Molecular Systems, Springfield Ave, Australia). β-Actin was used as a housekeeping gene. The qRT-PCR parameters employed and primer sequences are shown in Supplementary Table 1.

2.7. Scratch assay

A scratch assay was used to assess capacity for tumor cell motility. Briefly, 1 X 10^5 cells were seeded in 24-well plates and cultured overnight. On reaching confluency, the cell layer was scratched with a sterile plastic tip and then washed with culture medium twice and cultured again with the conditions previously described for up to 24 and 48 h (n=3). Representative images of the plates were taken under a microscope. The gap closure was measured by ImageJ analysis, by measuring the total area of cells in the gap.

2.8. 3D culture

PC-3 cells were seeded in bone-like scaffolds as described in Ref. [38]. Briefly, collagen/nano-hydroxyapatite scaffolds were produced and sterilized as described in Ref. [38] and then, 3 X 10^5 cells were seeded on them. 3D cultures were maintained in culture during 6 days, changing the RPMI medium each 3 days. After that, they were exposed to PCM treated during 60 s, to DOX 10 μM and with combination up to day 9 (n=3).

2.9. Cell viability in 3D models

After 9 days of cell culture, dsDNA and mRNA of each sample were isolated employing AllPrep DNA/RNA Mini Kit (Qiagen, 80204). For dsDNA determination, Quant-iT™ PicoGreen ® dsDNA Kit (Invitrogen, #P11496) was employed. dsDNA samples were diluted 1:10 in 1X TE buffer. 100 μL diluted sample were incubated with 100 μL PicoGreen® reagent (1:1) and incubated 5 min using dark flat-bottomed 96-well plate. The fluorescence was read at λex/em of 485/525 nm. Each value was referenced to control. mRNA expression were evaluated as previously described. For cell imaging in the scaffold, 3D models were incubated with Calcein AM and confocal images were captured using Zeiss laser scanning microscope.

2.10. Colony formation assay

To determine cell clonogeneity from 3D models after treatment, surviving cells of 3D models were isolated as described in Ref. [38]. Then, for colony formation assay, 2.5 X 10^3 cells/well were seeded in 6-well plate in their corresponding medium and then they were growth for 14 days, changing the medium each 3 days. After that, they were fixed and stained with Crystal Violet. Colony growth area were quantified by image analysis employing ImageJ and expressed aas fold change of control.

2.11. Co-culture assay

PC-3 cells were co-cultured both with hBM-MSCs and hObs. To identify each type of cells in the co-culture, PC-3 were labelled with CellTracker™ Blue CMAC Dye and hBM-MSCs or hObs were labelled with CellTracker™ Green CMFDA Dye (both from Invitrogen™) by incubating cells with their corresponding dye at final concentration of 25 μM in culture media. After that, cells were centrifuged, washed and resuspended in their corresponding culture media. Mixtures of PC-3 with hBM-MSCs or hObs at a proportion of 1:1 were seeded and treated as previously described. Representative images were taken after 24 and 72 h of treatment by using Zeiss laser scanning microscope. Cell amount was evaluated by image analysis using ImageJ, measuring blue-stained area for PC-3 and green-stained area for hBM-MSCs or hObs (4 pictures per sample, n=3).

2.12. Statistical analysis

All data are presented as means ± standard deviation (SD). Statistical analysis of the data was performed using ANOVA to compare conditions within the same experimental group and Student's t-test to compare couple of conditions between them. P-values < 0.05 were considered statistically significant.

3. Results

3.1. Plasma treatment and Plasma Conditioned Medium improve the anticancer effects of doxorubicin

kINPen ® IND was employed to produce direct CAP or PCM to treat PC-3 cells under the same operational parameters. The evaluation of cell toxicity in treatment time–response experiments showed that both CAP and PCM induced higher cytotoxic effect with higher treatment times (Fig. 1a). In addition, increasing concentrations of H_2O_2 and NO_2^- were also produced in PCM with treatment time (Supplementary Table 2). PC-3 cells were more sensitive to treatment with direct CAP (IC_{50} 17.14 s) than to PCM (IC_{50} 30.13 s) (Fig. 1a). As expected, PC-3 cells were moderately sensitive to DOX (Fig. 1b). Notably, the combination of PCM or CAP with DOX, especially at concentrations above 1 μM, markedly increased their cytotoxicity (Fig. 1b). In particular, in the combination, PCM and CAP shifted the IC50 of DOX in PC-3 cells from 8.3 to 1.5 μM and 1.1 μM respectively (Fig. 1b). Considering these similar values and the greater applicability of PCM in a future clinical scenario of metastatic bone cancer, for the following experiments only PCM is considered.

To further investigate the mechanism underlying the antiproliferative effect of this combination (PCM + DOX), we examined the accumulation of intracellular ROS and the cellular DOX uptake. We found that the combination of DOX (10 μM) and PCM (30 s) increased significantly the intracellular ROS from 0.5 h up to 2 h post treatment with respect to PCM or DOX separately (Fig. 1c), and the same trend was recorded for DOX uptake in PC-3 cells (Fig. 1d). We also evaluated the role of PCM and DOX over ABC pumps (drug transporters), by analyzing their mRNA levels. DOX treatment alone resulted in a non-significant regulation of *ABC* pumps, while PCM – 30 s alone or in combination with doxorubicin efficiently decreased the levels of *ABCC1*, *ABCB1* and *ABCG2* (Fig. 1e). Then, we also studied the expression of antioxidant genes Glutathione Peroxidase-1 (*GPX1*), Superoxide Dismutase 2 (*SOD2*) and Catalase 1 (*CAT1*). PCM did not greatly modulate their expression, while DOX significantly decreased the expression of antioxidants *SOD2* and *CAT1* (Fig. 1e). It should be noted that the combination of PCM with DOX significantly decreased the expression of all antioxidants and multi-drug resistance genes compared with DOX alone (Fig. 1e).

For further investigation on the mechanism underlying the anticancer effect of the combination of PCM and DOX, we examined their

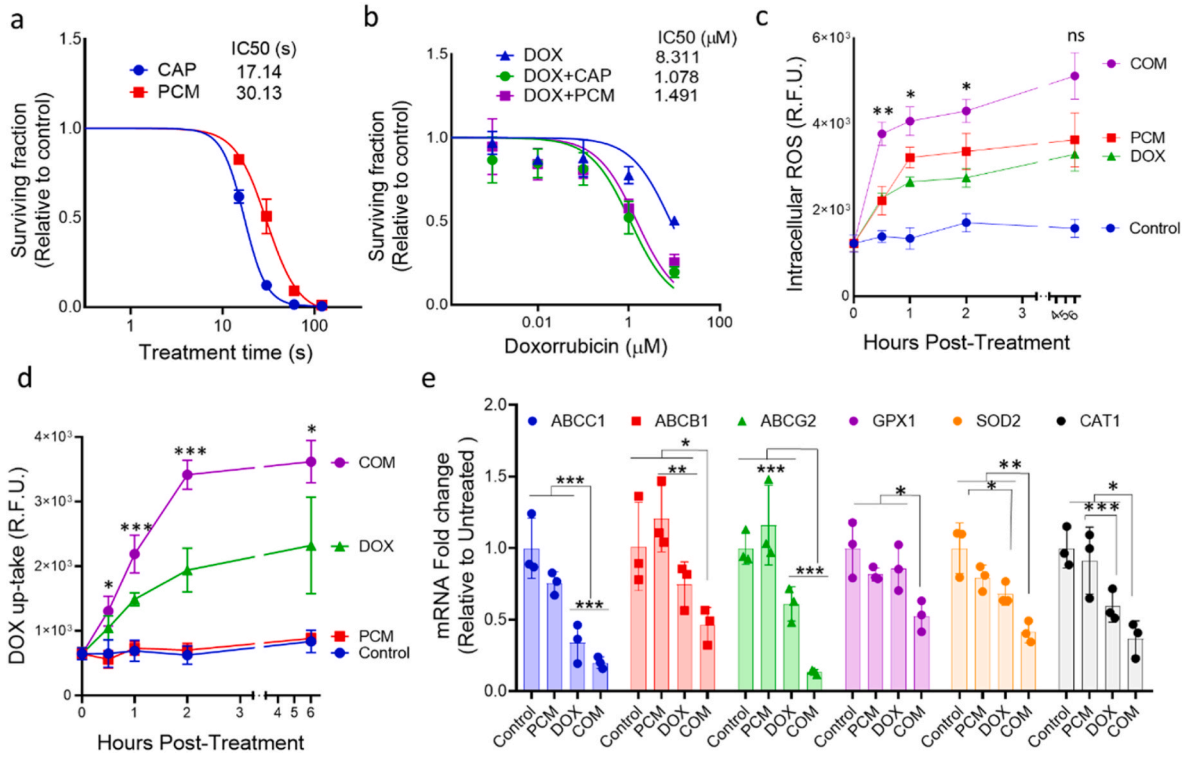

Fig. 1. Anti-proliferative effects of PCM and DOX in monolayer cultures. CAP was used to treat PC-3 cells in culture for times from 15 to 120 s or to obtain PCM, under the same operational parameters, that was then put in contact with them. a) Cell viability (WST-1 assay) on PC-3 cells was measured 72 h after exposure to CAP and PCM. IC50 values of CAP and PCM are shown in seconds. b) Cell viability curves representing the IC50 shift observed after 24 h of treatment of PC-3 with DOX alone or in combination with IC50 of CAP or PCM. Cell viability was expressed relativized to untreated control and is the mean and standard deviation (SD) of four independent experiments. c) Intracellular ROS measurement; PC-3 cells were pre-treated with dichlorofluorescein diacetate (DCFH-DA) at 40 μM during 1h. After that, cells were washed and exposed to culture medium (control), to PCM – 30 s, to DOX 10 μM and combination of both. Intracellular fluorescence is represented on the indicated treatment times after exposure to PCM, DOX or a combination of both (COM). d) Intracellular fluorescence of DOX was measured on the indicated treatment times after exposure to same conditions than before. Both experiments are expressed as Relative Fluorescence Units (RFU). Asterisk represented significant differences of combinatory treatment vs PCM or DOX separately. (* p-value < 0.05; ** p-value < 0.01; *** p-value < 0.005; two-sided two-way ANOVA). e) The mRNA levels modulated by of DOX (10 μM), PCM – 30 s and combination of both were determined by qRT-PCR of the indicated genes measured at 24 post-treatment in PC-3 cells. β-Actin was used as housekeeping gene. Data are represented as mean, n=3. Error bars represent SD and asterisks indicate statistically significant differences relativized to control (*p < 0.05; **p < 0.01, ***p < 0.001; two-sided Student's t-test). β-Actin levels were used as housekeeping.

effect on DNA damage and apoptosis induction. Both treatments separately (Fig. 2a–b) showed a potent induction of double-strand breaks in PC-3 cells as indicated by intranuclear γH2AX foci, and this effect was not observed to be significantly enhanced in the combination (Fig. 2a-b). In contrast, PC-3 displayed a similar apoptotic activation of BAX/BCL2 ratio after DOX and PCM treatment, but it was significantly enhanced (approximately 7-fold) in the combination (Fig. 2c).

Given the metastatic origin of PC-3 cells, we used a scratch assay to unravel whether PCM and DOX treatments could affect their cell migration ability. Microscope images showed that PCM seemed to slightly decrease cell migration compared to control, while DOX notably decreased PC-3 cells motility (Fig. 3a). Interestingly, PCM + DOX seemed to increase the anti-migratory effect of DOX at 48 h (Fig. 3a-b). This trend is confirmed by image analysis, where significant differences were found between DOX and COM at 48 h (Fig. 3b). In addition, qRT-PCR analysis of matrix metalloproteinases *MMP2* and *MMP9* confirmed that the combination significantly decreased the expression of MMP more efficiently than PCM or DOX alone (Fig. 3c).

3.2. PCM combined with DOX target metastatic cells in a 3D engineered model

Here, we employed a biomimetic bone scaffold composed by collagen type I and nano-hydroxyapatite (Col1/nHA) [23] that mimics the bone composition to culture PC-3 and evaluate the effectiveness of PCM + DOX in a more complex scenario. PC-3 cells were seeded in Col1/nHA scaffolds and they were grown in culture conditions prior to treatment. The 3D models were exposed to PCM – 60 s, DOX 10 μM and the combination of both for 3 days. To assess cell viability, we used Calcein AM staining of living cells (Fig. 4a), and Picogreen assay (Fig. 4b). Notably, only the combination treatment was able to reduce significantly cell viability (Fig. 4a–b) and as observed in monolayer, the combination improved the induction of apoptosis in 3D at transcriptional level measured as BAX/BCL2 ratio (Fig. 4 c).

Furthermore, to evaluate the clonogenic potential of PC-3 seeded into Col1/nHA, the 3D models were pre-treated for 72 h and the surviving cells were recovered to perform a colony formation assay (Fig. 4d-e). Representative images of colonies showed that neither PCM nor DOX were able to modify significantly the number of colonies (Fig. 4d). In contrast, we found a significant reduction of the area covered by the colonies obtained from 3D models exposed to the combination treatment (Fig. 4e). In line with these data, we also analyzed the transcriptional profile of 3D cultures, and we found that PCM + DOX were able to decrease significantly the drug-resistant phenotype, decreasing the expression of *ABCC1*, *ABCB1* and *ABCG2* at transcriptional levels and coupled to a downregulation of the anti-oxidant defenses *GPX1*, *SOD2*, and *CAT1*.

3.3. The combination therapy selectively targets prostate cancer cells

To study the selective effect of PCM + DOX, first the effect of PCM – 30 s, DOX 10 μM or a combination on cell viability were evaluated in PC-

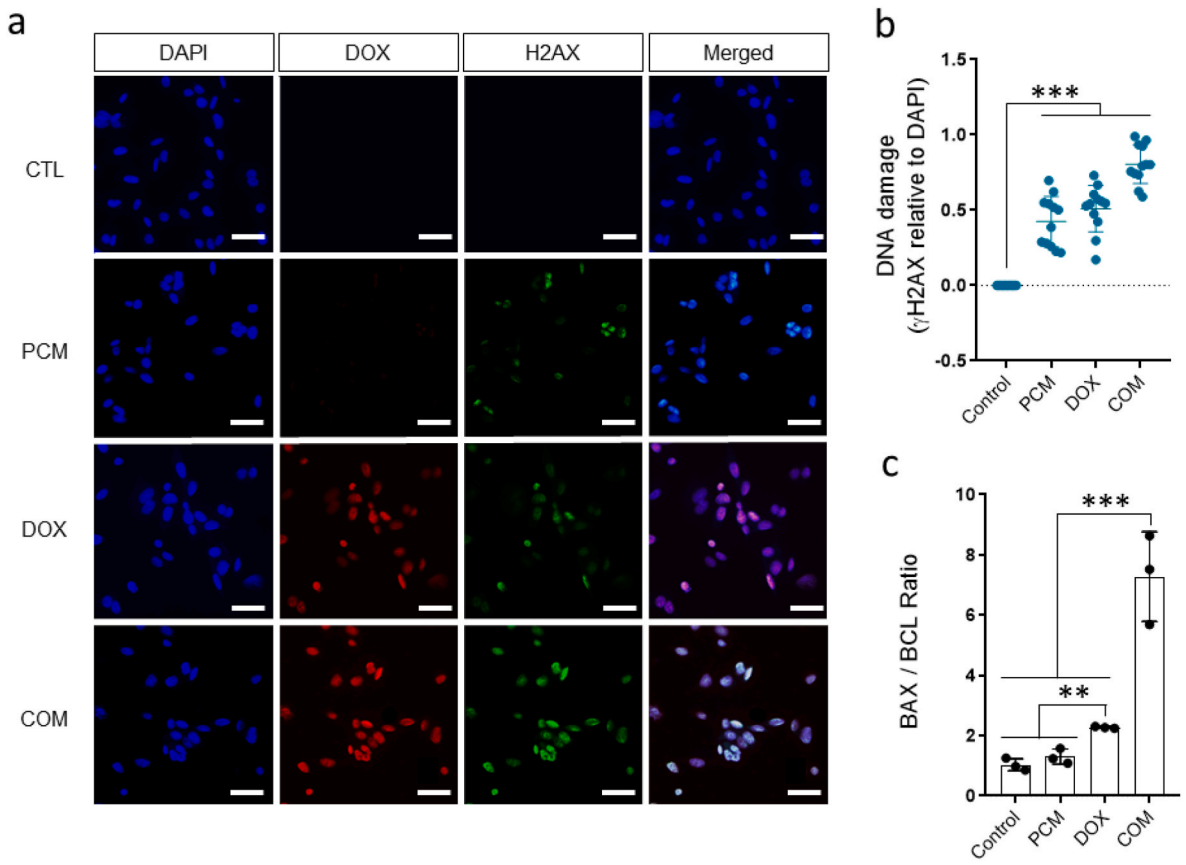

Fig. 2. DNA damage and apoptosis induced by PCM and DOX. a) PC-3 cells exposed to culture medium (CTL), PCM-30s, DOX 10 μM and PCM-30s + DOX 10 μM were fixed and immunostained for γH2AX and representative images were taken by confocal microscopy. Scale bar: 50 μm. b) DNA damage quantification (positive γH2AX area relativized to DAPI area; n = 3, 6 images per sample).c) qRT-PCR of BAX and BCL2, expressed as BAX/BCL2 ratio. Values were relativized to control and expressed as fold change (n=3, mean + SD). Data as presented as mean and standard deviation of n=3 replicates (* p-value < 0.05; ** p-value < 0.01; *** p-value < 0.005; two-sided Student's t-test).

3 cells, hBM-MSCs and hObs 24h and 72h post-treatment. Cell viabiliy analysis showed a slight decrease of cell viability in non-malignant hBM-MSCs or hOBs treated with PCM – 30 s, DOX 10 μM or a combination of both for 24 h post-treatment (Fig. 5a, left). However, 72 h post-treatment we found that DOX and DOX + PCM affect the cell viability of non-malignant cells (Fig. 5a, right). Importantly, the combined treatment boosted the ability of PCM and DOX to abolish cell viability preferently in PC-3 without important effects in non-malignant cells (Fig. 5a) when compared to the single treatment with DOX. To obtain more insights on this selective anti-tumor effect of the combination, we performed co-cultures in monolayer by seeding bone non-malignant cells with PC-3 cells. Representative images of the co-cultures revealed similar morphologies in hBM-MSCs at 24 h in all conditions (Fig. 5b), and smaller cell areas with less visible amount of PC-3 cells exposed to COM compared with CTL (Fig. 5b). Concordantly, the cell tracking by fluorescence revealed that the combinatory treatment targeted preferently PC-3 cells (Fig. 5c) than hBM-MSCs. A similar trend was found in co-cultures employing hOBs, where the combination preferently eliminated PC-3 with respect to hOBs (Fig. 5d–e). Overall, we show evidence that PC-3 cells treated with a combination of DOX + PCM were significantly and selectively affected while non-malignant cells were clearly less affected (Fig. 5).

4. Discussion

Metastasis is responsible for most of cancer-related morbidity and mortality, being bones one of the prominent organs that suffer from the metastatic spread of cancer. In breast and prostate cancers, it is estimated that >70% of late-stage patients develop skeletal metastases [39]. The existing approach for the treatment of bone metastases is the use of high-dose chemotherapy, but there are no real curative options and they are associated with harmful side effects [40,41]. In the research for alternative treatments of cancer, CAP and PCL have shown equivalent anti-cancer effects in bone [30] and prostate cancer [42–46], among other cancer types [11]. Moreover, CAP and PCL have shown to enhance drug uptake, which is often attributed to similar effects to electroporation, leading to enhanced membrane permeability that increase the anti-cancer effect of drugs [22,25,26]. However, most of these studies have been performed in monolayer cultures, which obviate many relevant aspects for clinical translation.

Here, by using three different models: 2D monolayers, 3D bone bioengineered tumors and co-cultures of malignant and non-malignant cells, we have been able to reach important findings: i. fostered effects of DOX internalization thanks to PCL, which are associated to reduced expression of ABC pumps and of the antioxidant defenses; ii. a clearly reduced cell migration capacity in the combined therapy, which decrease the expression of matrix metalloproteinases, and; iii. that the bone microenvironment enhances the cell resistance to the treatment, but the combined treatment is able to successfully reduce the clonogenic capacity of the cells. These findings indicate a reduced metastatic ability of the treated cancer cells in this context. Lastly, the simultaneous co-therapy of non-malignant and malignant cells clearly showed the selective effect of the treatment. In the next paragraphs we dive into these findings in more detail.

Firstly, regarding DOX; We selected this anthracycline drug because it is one of the most potent antineoplasic drugs and very often used in the

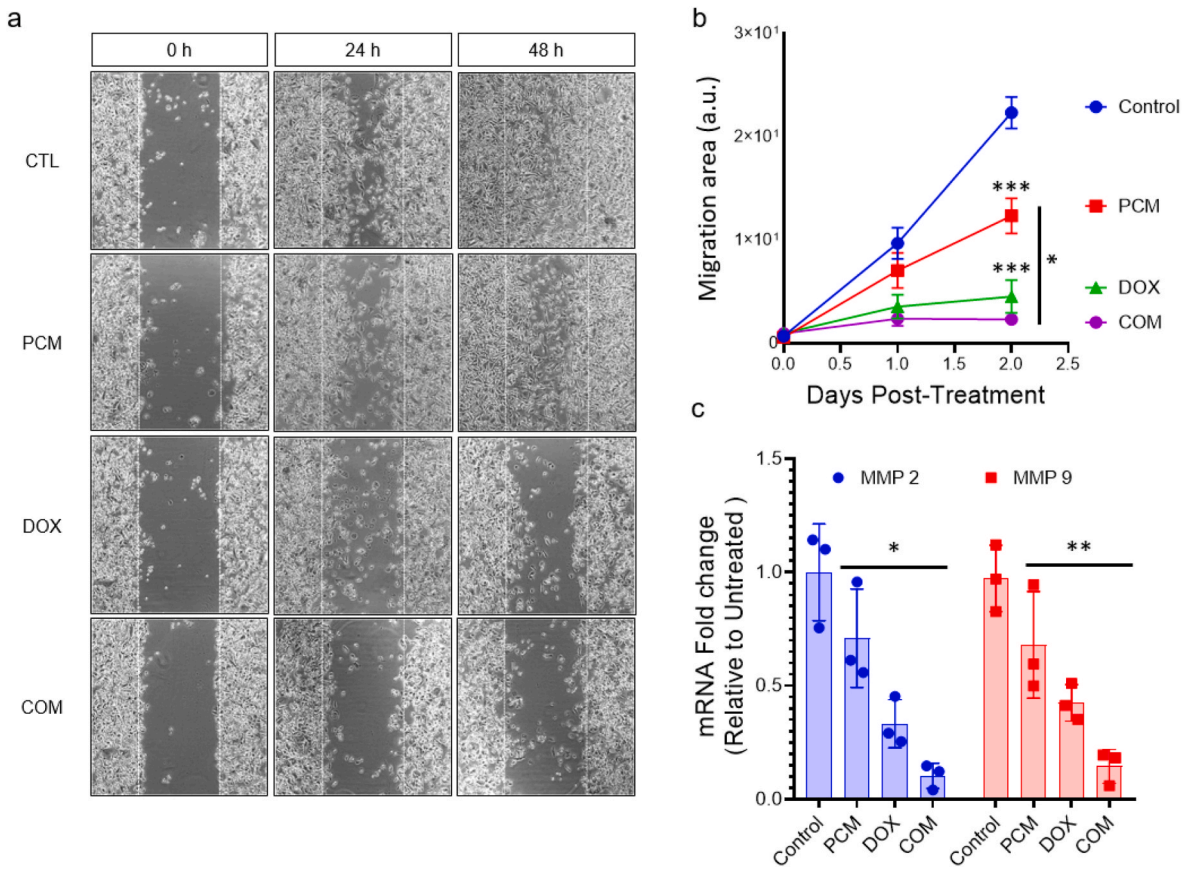

Fig. 3. Effect of PCM and DOX on cell migration of PC-3 cells. a) Representative images of the wound healing assay in the different conditions 0, 24 and 48 h after treatment (4X). b) Migration area determined by image analysis of the total area of cells in the scratched area 24 and 48 h after treatment, expressed in arbitrary units (n=3, mean + SD). c) RT-PCR of cell motility genes MMP-2 and MMP-9 from cells after 24 h of treatment. Values were relativized to control and expressed as fold change (n=3, mean + SD). Asterisk represented significant differences between COM and PCM or DOX separately (* p-value < 0.05; ** p-value < 0.01; *** p-value < 0.005; two-sided Student's t-test).

management of metastatic bone cancers. Unfortunately, injury to non-targeted tissues often complicates cancer treatment by limiting therapeutic dosages of DOX and diminishing the quality of patients' life [4]. Today, different strategies are under investigation concerning the management of DOX-induced toxicity, still with limited success. For this reason, exploring new therapeutic options to improve the anti-tumoral activity of DOX is an urgent need. Encouraging results demonstrated that direct CAP application increases the delivery effectiveness of drug nanocarriers in glioblastoma [47] or melanoma [48], and of free chemotherapeutic agents (temozolomide) in glioblastoma cells [20] or cisplatin in squamous cell carcinoma [28]. This enhanced drug delivery has often been ascribed to the electromagnetic fields present in CAP - similar to electroporation - despite the main anticancer effects of CAP are attributed to oxidative stress. However, CAP faces limitations to be applied to tumors in internal organs like bone cancers [30], so employing PCM where RONS can be generated by CAP treatment is an interesting approach (Suppl. Table 2) that we combined with DOX to investigate whether PCM can be an alternative to enhance DOX toxicity against PC-3 cells. Here, both direct CAP application and PCM at IC50 (Fig. 1a) significantly increased the DOX cytotoxicity (Fig. 2b). The combination of PCM with the drug increased the levels of intracellular ROS more than DOX or PCM alone (Fig. 1c) and PCM improved the uptake of DOX (Fig. 1d).

Induction of oxidative stress is one of the effects mediated by DOX and the main mechanism of PCM to induce cancer cell death [36,37]. Here, the great cytotoxic potential of PCM + DOX was related to the disruption of cancer antioxidant defenses; We analyzed the levels of GPX1, which scavenges ROS like $OHOO^-$ and H_2O_2 to form H_2O; mitochondrial SOD2, an enzyme that eliminates O_2^-; and CAT1, which acts as H_2O_2 scavenger. PCM and DOX downregulated moderately the expression of antioxidant genes like *SOD2*, *GPX1* and *CAT1*, but this effect was strongly powered in the combination of both (Fig. 1e). Moreover, we analyzed the expression of well-recognized ABC pumps *ABCC1*, *ABCB1* and *ABCG2* (Fig. 1e) associated to DOX resistance [34], which were found to significantly decrease in the combined treatment. This is relevant because the downregulation of this ABC pumps increases the effectiveness of DOX in cancer [49,50].

To clarify the cell death mechanism, we analyzed the levels of apoptosis by evaluating the transcriptional levels of BAX/BCL2. First, we found that the PCM + DOX combination substantially increases DNA damage (Fig. 2a–b) and overall the combinatory treatment enhanced the pro-apoptotic signalling (Fig. 2c). Our data clearly confirm that PCM increases the intracellular oxidative damage of DOX, by increasing its uptake in PC-3 cells and interfering in their antioxidant defences and drug efflux transporters that results in an apoptosis induction. These results are particularly interesting, as the enhanced uptake found here with PCM had mainly been attributed to electromagnetic fields from CAP, so our findings allow to conclude on the important role played by RONS in PCL on these effects, and open thus a new research pathway, more suitable for local therapy by injection.

Secondly, the combined effect of PCM + DOX showed better capacity to inhibit cell migration in comparison with only DOX (Fig. 3). This observation is substantiated by previous studies that have reported a decrease in the rate of cell migration after CAP treatment in prostate cancer cells [42,43,45]. In addition to this, the combined treatment also enhanced the down-regulation already induced by DOX in the

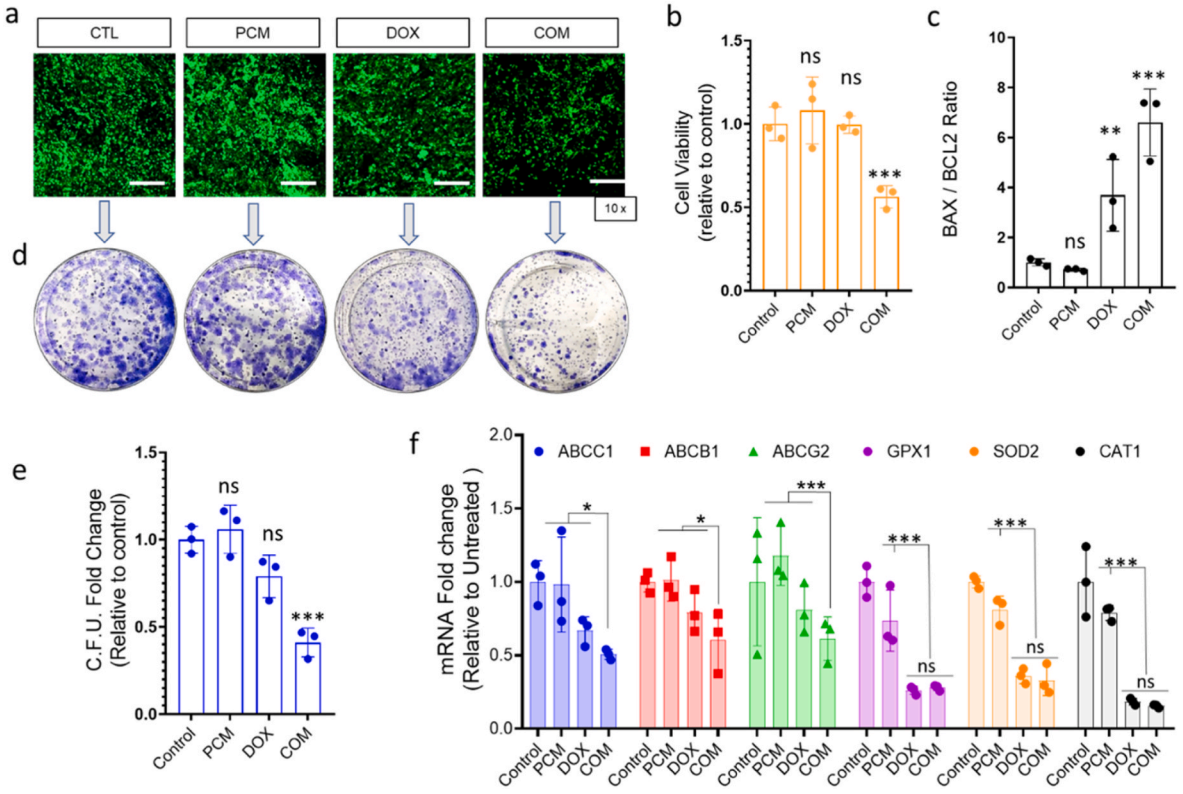

Fig. 4. Effects of PCM and DOX in prostate cancer 3D engineered model. PC-3 cells were seeded onto Col1/nHA scaffolds and allowed to growt during 6 days. a) Representative images of 3D models treated during 72 h on the indicated treatments stained with Calcein AM. Scale bars = 200 μm b) The antiproliferative effects of DOX 10 μM, PCM – 60 s and combination of both were determined by Picogreen assay on 3D cultures of PC-3, 72 h post-treatment. Cell viability is represented as relative to untreated (control) 3D cultures. c) qRT-PCR of BAX and BCL2, expressed as BAX/BCL2 ratio. Values were relativized to control and expressed as fold change (n=3, mean + SD). d) To assay the clonogenic potential of surviving PC-3 cells, 72 h pre-treatments of PCM – 60 s, DOX 10 μM and combination of both were performed in 3D cultures. Then, cells were recovered from the 3D models and re-seeded at a density of 2.5 X 10^3 cells in 6-well plates up to 14 days. d) Representative images of the colonies formed and e) quantification of the area covered by the colonies. Data are presented relativized to control. Data are presented as mean, n=3. f) The mRNA levels modulated by DOX (10 μM), PCM – 60 s and combination of both were determined by qRT-PCR of the indicated genes measured at 72 post-treatment. β-Actin was used as housekeeping gene. Data are represented as mean, n=3. Error bars represent SD and asterisks indicate statistically significant differences relativized to control (*$p < 0.05$; **$p < 0.01$, ***$p < 0.001$; two-sided Student's t-test).

expression of *MMP-2* and *MMP-9* genes, which are related with cell motility (Fig. 3c). Taken together, these data may suggest that the oxidative stress induced by PCM could enhance the anti-migratory effect of DOX in PC-3, thus diminishing their metastatic ability.

In the third place, despite all these interesting findings described in 2D, it is widely acknowledged that the lack of the 3D tumor microenvironment is related to monolayer cultures being less good predictors of the responses to anti-cancer therapies [51]. Considering that, to the best of our understanding, there are no preclinical 3D models demonstrating the beneficial effects of combinatory treatments in metastatic bone cancers, we developed a 3D engineered tumor model from PC-3 seeded into Col1/nHA scaffolds. The bone environment acts as barrier for drug diffusion of chemotherapeutic agents and this effect is particularly relevant in the management of bone cancers [52]. In a previous work exploring osteosarcoma, we found that cold-plasma-based therapies were much less efficient in a 3D engineered model due its ability to scavenge ROS and support stem cell properties [38]. For these reasons, in addition to the 10-fold higher amount of initial cells in 3D versus 2D, the assays performed in the 3D models employed longer plasma treatment times to generate the PCM (PCM-60s) than those performed in monolayer.

Here, the engineered metastatic PC-3 tumors presented high resistance to PCM and DOX despite they were treated with twice the concentration of RONS in PCM with respect to the one used in 2D cultures. Moreover, the combination of PCM + DOX was only able to reduce 50% of cell viability (Fig. 4a-b). The transcriptional analysis of the tumor model showed that only the combination treatment was able to target drug-resistant and antioxidant genes (Fig. 4f), and overall only in the combination we recorded a significant reduction of the clonogenic ability (Fig. 4d-e).

Lastly, beyond the enhanced cytotoxic targeting of prostate metastatic cells effects found in the combination of PCM + DOX, it is necessary to evaluate the capacity of this combination to avoid undesirable side-effects on non-malignant cells. This was done in mono- and co-cultures of PC-3 with non-malignant bone cells (mesenchymal stem cells and osteoblasts). In monoculture, we found that PCM + DOX preferently targeted cancer cell viability without increasing the cytotoxic effect of DOX in healthy cells (Fig. 5a). Similar trends were observed in co-culture experiments, where the combination of PCM + DOX increased the cytotoxic effects on PC-3 without affecting the morphology of hBM-MSCs nor hObs and with minor effects on their viability (Fig. 5). Several studies suggested that metastatic cancers can inhibit osteblasts and bone cell precursors and stimulate osteoclastic activity in order to accommodate bone tumor formation [53–56]. In this way, targeting prostate cancer cells by combined PCM + DOX treatment could counteract the bone destruction induced by metastatic tumors.

5. Conclusion

This is the first work describing the combined effects of PCM and DOX as a promising option to improve the therapeutics of prostate metastatic bone cancer. The oxidative stress delivered by PCM enhanced

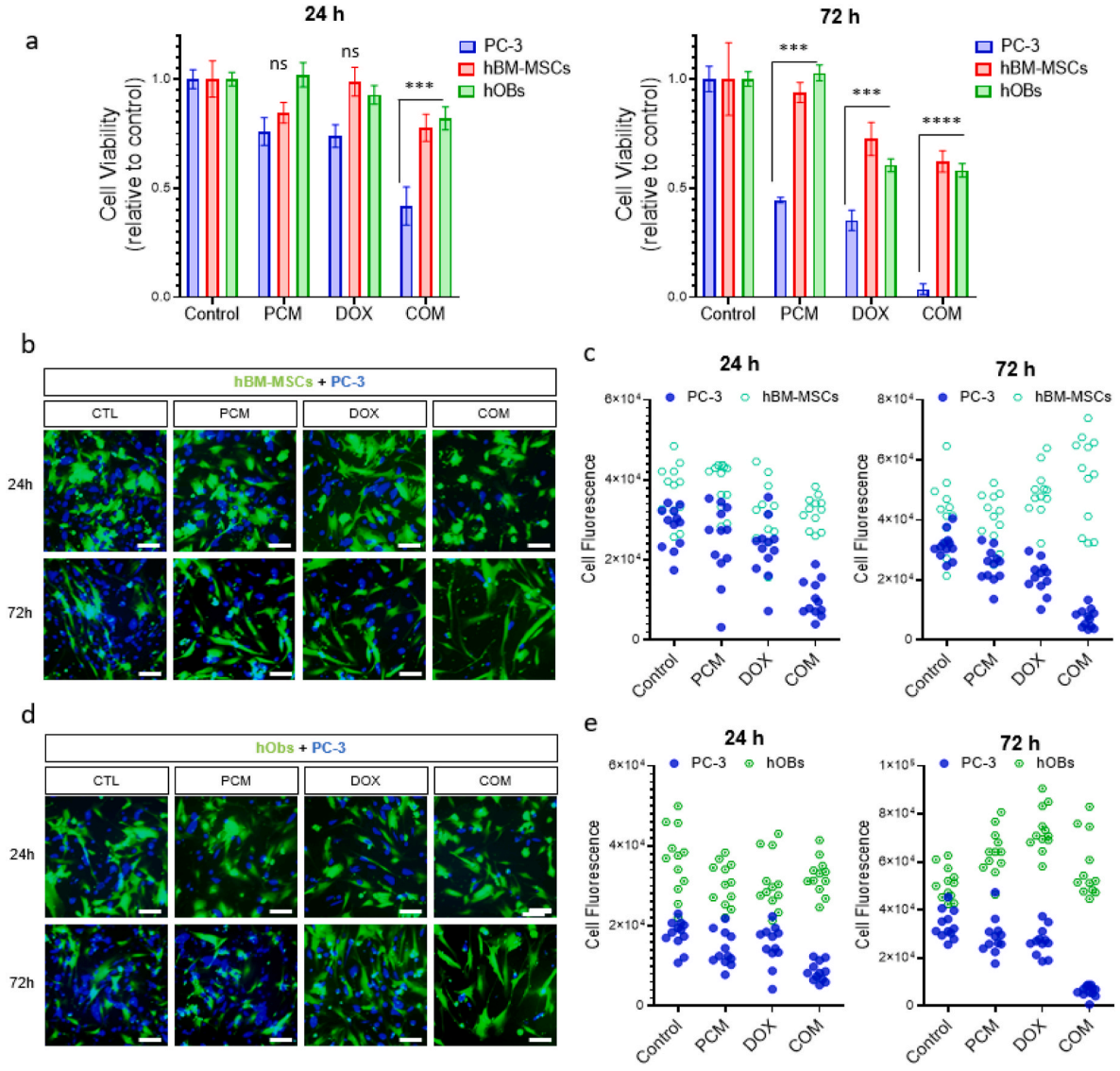

Fig. 5. Anti-cancer selectivity of PCM + DOX. a) Effects of PCM – 30 s, DOX (10 μM) and combination (COM) on cell viability were quantified by WST-1 assay in monolayer on hBM-MSCs, hOBS vs cancer PC-3 cells, measured 24 h after exposure (left panel) or 72h (right panel). Cell viability is expressed relative to the corresponding untreated control and is the mean and standard deviation of three independent experiments (*p < 0.05; **p < 0.005; two-sided Student's t-test). Co-cultures of non-malignant cells (marked in green fluorescence) and PC-3 (marked in blue fluorescence) were treated by PCM, DOX or combination over b-c) hBM-MSCs + PC-3 or d-e) hOBs + PC-3 during 24 h and 72 h. Scale bar: 100 μm. Cell viability of hBM-MSCs + PC-3 co-cultures c) 24 h and d) 72 h post-treatment and of hObs + PC-3 co-cultures e) 24 h and f) 72 h. Cell tracking was determined by fluorescence analysis, expressed in arbitrary units (4 images per condition, n=3). Asterisk represented significant differences (* p-value < 0.05; ** p-value < 0.01; *** p-value < 0.005; two-sided Student's t-test). (For interpretation of the references to colour in this figure legend, the reader is referred to the Web version of this article.)

the uptake of DOX by PC-3 cells, increased the intracellular oxidative stress and led to apoptosis. Antioxidant and drug-resistant gene transcription was specifically downregulated by the combined treatment, as was the migration capacity of PC-3 cells. The efficacy of the treatment, enhanced apoptosis and targeting of ABC pumps was confirmed by developing a 3D tumor engineered model and thus in the presence of a surrounding bone-like ECM. Furthermore, PCM selectively improved the targeting of DOX towards PC-3 cells versus non-malignant bone cells, which could be a useful approach to overcome undesirable side-effects and reduce the effective dose of DOX. Overall, this work opens a new avenue to improve the specificity and efficiency of DOX for metastatic bone cancer treatment by combining it with an oxidative-stress based, injectable therapy: plasma-conditioned liquids.

Author contributions

MM and JT conceived the project and designed experiments; MM performed experiments and analyzed data; MM and JT wrote the manuscript. CC & MPG contributed to the review of the manuscript; supervised the study & obtained funding.

Conflicts of interest

The authors declare that there is no conflict of interest.

8.Acknowledgements

This project has been primarily funded from the European Research Council (ERC) under the European Union's Horizon 2020 research and innovation program (grant agreement No. 714793). The authors

acknowledge MINECO for PID2019-103892RB-I00/AEI/10.13039/501100011033 project. The authors belong to SGR2017-1165. Authors acknowledge Generalitat de Catalunya for the Scholarship of MM (2020 FI-B00999). MPG and CC acknowledge the ICREA Academia Award for Excellence in Research, funded by the Generalitat de Catalunya.

Appendix A. Supplementary data

Supplementary data to this article can be found online at https://doi.org/10.1016/j.freeradbiomed.2022.07.007.

References

[1] F. Macedo, K. Ladeira, F. Pinho, N. Saraiva, N. Bonito, L. Pinto, F. Gonçalves, Bone metastases: an overview, Onco Rev. 11 (2017), https://doi.org/10.4081/oncol.2017.321.

[2] A.E. Bădilă, D.M. Rădulescu, A.-G. Niculescu, A.M. Grumezescu, M. Rădulescu, A. R. Rădulescu, Recent advances in the treatment of bone metastases and primary bone tumors: an up-to-date review, Cancers 13 (2021) 4229, https://doi.org/10.3390/cancers13164229.

[3] M.B. Meads, L.A. Hazlehurst, W.S. Dalton, The bone marrow microenvironment as a tumor sanctuary and contributor to drug resistance, Clin. Cancer Res. 14 (2008) 2519–2526, https://doi.org/10.1158/1078-0432.CCR-07-2223.

[4] C. Carvalho, R. Santos, S. Cardoso, S. Correia, P. Oliveira, M. Santos, P. Moreira, Doxorubicin: the good, the bad and the ugly effect, Curr. Med. Chem. 16 (2009) 3267–3285, https://doi.org/10.2174/092986709788803312.

[5] P. Brun, G. Bernabè, C. Marchiori, M. Scarpa, M. Zuin, R. Cavazzana, B. Zaniol, E. Martines, Antibacterial efficacy and mechanisms of action of low power atmospheric pressure cold plasma: membrane permeability, biofilm penetration and antimicrobial sensitization, J. Appl. Microbiol. 125 (2018) 398–408, https://doi.org/10.1111/jam.13780.

[6] K.A. Lis, C. Kehrenberg, A. Boulaaba, M. von Köckritz-Blickwede, S. Binder, Y. Li, J. L. Zimmermann, Y. Pfeifer, B. Ahlfeld, Inactivation of multidrug-resistant pathogens and Yersinia enterocolitica with cold atmospheric-pressure plasma on stainless-steel surfaces, Int. J. Antimicrob. Agents 52 (2018) 811–818, https://doi.org/10.1016/j.ijantimicag.2018.08.023.

[7] F. Tan, X. Rui, X. Xiang, Z. Yu, M. Al-Rubeai, Multimodal treatment combining cold atmospheric plasma and acidic fibroblast growth factor for multi-tissue regeneration, Faseb. J. (2021) 35, https://doi.org/10.1096/fj.202002611R.

[8] M.R. Amini, M. Sheikh Hosseini, S. Fatollah, S. Mirpour, M. Ghoranneviss, B. Larijani, M.R. Mohajeri-Tehrani, M.R. Khorramizadeh, Beneficial effects of cold atmospheric plasma on inflammatory phase of diabetic foot ulcers; a randomized clinical trial, J. Diabetes Metab. Disord. 19 (2020) 895–905, https://doi.org/10.1007/s40200-020-00577-2.

[9] Z. Xiong, S. Zhao, X. Yan, Nerve stem cell differentiation by a one-step cold atmospheric plasma treatment in vitro, JoVE (Journal Vis. Exp. 2019 (2019), e58663, https://doi.org/10.3791/58663.

[10] Y. Nomura, T. Takamatsu, H. Kawano, H. Miyahara, A. Okino, M. Yoshida, T. Azuma, Investigation of blood coagulation effect of nonthermal multigas plasma jet in vitro and in vivo, J. Surg. Res. 219 (2017) 302–309, https://doi.org/10.1016/j.jss.2017.06.055.

[11] A. Dubuc, P. Monsarrat, F. Virard, N. Merbahi, J.-P. Sarrette, S. Laurencin-Dalicieux, S. Cousty, Use of cold-atmospheric plasma in oncology: a concise systematic review, Ther. Adv. Med. Oncol. 10 (2018), 1758835918786475, https://doi.org/10.1177/1758835918786475.

[12] H.R. Metelmann, C. Seebauer, V. Miller, A. Fridman, G. Bauer, D.B. Graves, J. M. Pouvesle, R. Rutkowski, M. Schuster, S. Bekeschus, et al., Clinical experience with cold plasma in the treatment of locally advanced head and neck cancer, Clin. Plasma Med. 9 (2018) 6–13, https://doi.org/10.1016/j.cpme.2017.09.001.

[13] S.U. Kang, J.H. Cho, J.W. Chang, Y.S. Shin, K.I. Kim, J.K. Park, S.S. Yang, J.S. Lee, E. Moon, K. Lee, et al., Nonthermal plasma induces head and neck cancer cell death: the potential involvement of mitogen-activated protein kinase-dependent mitochondrial reactive oxygen species, Cell Death Dis. 5 (2014), https://doi.org/10.1038/cddis.2014.33.

[14] Y. Sato, S. Yamada, S. Takeda, N. Hattori, K. Nakamura, H. Tanaka, M. Mizuno, M. Hori, Y. Kodera, Effect of plasma-activated lactated ringer's solution on pancreatic cancer cells in vitro and in vivo, Ann. Surg Oncol. 25 (2018) 299–307, https://doi.org/10.1245/s10434-017-6239-y.

[15] H. Tanaka, K. Nakamura, M. Mizuno, K. Ishikawa, K. Takeda, H. Kajiyama, F. Utsumi, F. Kikkawa, M. Hori, Non-thermal atmospheric pressure plasma activates lactate in Ringer's solution for anti-tumor effects, Sci. Rep. 6 (2016), 36282, https://doi.org/10.1038/srep36282.

[16] J. Tornin, C. Labay, F. Tampieri, M.P. Ginebra, C. Canal, Evaluation of the effects of cold atmospheric plasma and plasma-treated liquids in cancer cell cultures, Nat. Protoc. 16 (2021) 2826–2850.

[17] Y. Li, T. Tang, H.J. Lee, K. Song, Selective anti-cancer effects of plasma-activated medium and its high efficacy with cisplatin on hepatocellular carcinoma with cancer stem cell characteristics, Int. J. Mol. Sci. (2021) 22, https://doi.org/10.3390/IJMS22083956.

[18] G.E. Conway, A. Casey, V. Milosavljevic, Y. Liu, O. Howe, P.J. Cullen, J.F. Curtin, Non-thermal atmospheric plasma induces ROS-independent cell death in U373MG glioma cells and augments the cytotoxicity of temozolomide, Br. J. Cancer 114 (2016) 435–443, https://doi.org/10.1038/bjc.2016.12.

[19] P. Shaw, N. Kumar, A. Privat-maldonado, E. Smits, A. Bogaerts, Cold atmospheric plasma increases temozolomide sensitivity of three-dimensional glioblastoma spheroids via oxidative stress-mediated dna damage, Cancers 13 (2021) 1780, https://doi.org/10.3390/CANCERS13081780/S1.

[20] E. Gjika, S. Pal-Ghosh, M.E. Kirschner, L. Lin, J.H. Sherman, M.A. Stepp, M. Keidar, Combination therapy of cold atmospheric plasma (CAP) with temozolomide in the treatment of U87MG glioblastoma cells, Sci. Rep. 10 (2020) 1–13, https://doi.org/10.1038/s41598-020-73457-7, 101 **2020**.

[21] J. Köritzer, V. Boxhammer, A. Schäfer, T. Shimizu, T.G. Klämpfl, Y.-F. Li, C. Welz, S. Schwenk-Zieger, G.E. Morfill, J.L. Zimmermann, et al., Restoration of sensitivity in chemo-resistant glioma cells by cold atmospheric plasma, PLoS One 8 (2013), e64498, https://doi.org/10.1371/journal.pone.0064498.

[22] K. Pefani-Antimisiari, D.K. Athanasopoulos, A. Marazioti, K. Sklias, M. Rodi, A.-L. de Lastic, A. Mouzaki, P. Svarnas, S.G. Antimisiaris, Synergistic effect of cold atmospheric pressure plasma and free or liposomal doxorubicin on melanoma cells, Sci. Rep. (2021) 11, https://doi.org/10.1038/S41598-021-94130-7.

[23] F. Utsumi, H. Kajiyama, K. Nakamura, H. Tanaka, M. Mizuno, K. Ishikawa, H. Kondo, H. Kano, M. Hori, F. Kikkawa, Effect of indirect nonequilibrium atmospheric pressure plasma on anti-proliferative activity against chronic chemo-resistant ovarian cancer cells in vitro and in vivo, PLoS One 8 (2013), https://doi.org/10.1371/journal.pone.0081576.

[24] V. Soni, M. Adhikari, H. Simonyan, L. Lin, J.H. Sherman, C.N. Young, M. Keidar, In vitro and in vivo enhancement of temozolomide effect in human glioblastoma by non-invasive application of cold atmospheric plasma, Cancers 13 (2021) 4485, https://doi.org/10.3390/CANCERS13174485/S1.

[25] K.-R. Liedtke, E. Freund, M. Hermes, S. Oswald, C.-D. Heidecke, L.-I. Partecke, S. Bekeschus, Gas plasma-conditioned ringer's lactate enhances the cytotoxic activity of cisplatin and gemcitabine in pancreatic cancer in vitro and in ovo, Cancers 12 (2020) 123, https://doi.org/10.3390/CANCERS12010123.

[26] S.K. Sagwal, G. Pasqual-Melo, Y. Bodnar, R.K. Gandhirajan, S. Bekeschus, Combination of chemotherapy and physical plasma elicits melanoma cell death via upregulation of SLC22A16, Cell Death Dis. 9 (2018), https://doi.org/10.1038/S41419-018-1221-6.

[27] S. Park, H. Kim, H.W. Ji, H.W. Kim, S.H. Yun, E.H. Choi, S.J. Kim, Cold atmospheric plasma restores paclitaxel sensitivity to paclitaxel-resistant breast cancer cells by reversing expression of resistance-related genes, Cancers 11 (2019), https://doi.org/10.3390/CANCERS11122011.

[28] C.-M. Lee, Y.-I. Jeong, M.-S. Kook, B.-H. Kim, Combinatorial effect of cold atmosphere plasma (CAP) and the anticancer drug cisplatin on oral squamous cell cancer therapy, Int. J. Mol. Sci. 21 (2020) 1–15, https://doi.org/10.3390/IJMS21207646.

[29] I.L. Ibañez, C. Notcovich, P.N. Catalano, M.G. Bellino, H. Durán, The redox-active nanomaterial toolbox for cancer therapy, Cancer Lett. 359 (2015) 9–19, https://doi.org/10.1016/J.CANLET.2015.01.013.

[30] M. Mateu-Sanz, J. Tornín, M.-P. Ginebra, C. Canal, Cold atmospheric plasma: a new strategy based primarily on oxidative stress for osteosarcoma therapy, J. Clin. Med. 10 (2021) 893, https://doi.org/10.3390/jcm10040893.

[31] A. Marturano-Kruik, A. Villasante, G. Vunjak-Novakovic, Bioengineered models of solid human tumors for cancer research, in: Methods in Molecular Biology, vol. 1502, Humana Press Inc., 2016, pp. 203–211.

[32] A. Villasante, G. Vunjak-Novakovic, Tissue-engineered models of human tumors for cancer research, Expet Opin. Drug Discov. 10 (2015) 257–268.

[33] A. De Luca, L. Raimondi, F. Salamanna, V. Carina, V. Costa, D. Bellavia, R. Alessandro, M. Fini, G. Giavaresi, Relevance of 3d culture systems to study osteosarcoma environment, J. Exp. Clin. Cancer Res. 37 (2018).

[34] S.T. Menéndez, B. Gallego, D. Murillo, A. Rodríguez, R. Rodríguez, Cancer stem cells as a source of drug resistance in bone sarcomas, J. Clin. Med. 10 (2021) 2621, https://doi.org/10.3390/jcm10122621.

[35] A. Abarrategi, J. Tornin, M.C. Lucia, A. Hamilton, M.C. Enrique, J.P. Rodrigo, M. V. González, N. Baldini, G.C. Javier, R. Rodriguez, Osteosarcoma: cells-of-Origin, Cancer stem cells, and targeted therapies, Stem Cell. Int. 2016 (2016).

[36] J. Tornin, M. Mateu-Sanz, A. Rodríguez, C. Labay, R. Rodríguez, C. Canal, Pyruvate plays a main role in the antitumoral selectivity of cold atmospheric plasma in osteosarcoma, Sci. Rep. 9 (2019), https://doi.org/10.1038/S41598-019-47128-1.

[37] M. Mateu-Sanz, J. Tornín, B. Brulin, A. Khlyustova, M.-P. Ginebra, P. Layrolle, C. Canal, Cold plasma-treated ringer's saline: a weapon to target osteosarcoma, Cancers 12 (2020) 227, https://doi.org/10.3390/CANCERS12010227. *Page 227* **2020**, 12.

[38] J. Tornín, A. Villasante, X. Solé-Martí, M.-P. Ginebra, C. Canal, Osteosarcoma tissue-engineered model challenges oxidative stress therapy revealing promoted cancer stem cell properties, Free Radic. Biol. Med. 164 (2021) 107–118, https://doi.org/10.1016/j.freeradbiomed.2020.12.437.

[39] H. Zheng, W. Li, Y. Kang, Tumor-stroma interactions in bone metastasis: Molecular mechanisms and therapeutic implications, Cold Spring Harbor Symp. Quant. Biol. 81 (2016) 151–161, https://doi.org/10.1101/sqb.2016.81.030775.

[40] R.E. Coleman, Metastatic bone disease: clinical features, pathophysiology and treatment strategies, Cancer Treat Rev. 27 (2001) 165–176, https://doi.org/10.1053/CTRV.2000.0210.

[41] J.L. Ferguson, S.P. Turner, Bone cancer: diagnosis and treatment principles, Am. Fam. Physician 98 (2018) 205–213.

[42] A. Zhunussova, E.A. Vitol, B. Polyak, A.D. Brooks, R. Sensenig, G. Friedman, Z. Orynbayeva, Mitochondria-Mediated Anticancer Effects of Non-Thermal Atmospheric Plasma, 2016, https://doi.org/10.1371/journal.pone.0156818.

[43] M. Weiss, D. Gümbel, E.M. Hanschmann, R. Mandelkow, N. Gelbrich, U. Zimmermann, R. Walther, A. Ekkernkamp, A. Sckell, A. Kramer, et al., Cold atmospheric plasma treatment induces anti-proliferative effects in prostate cancer cells by redox and apoptotic signaling pathways, PLoS One 10 (2015), https://doi.org/10.1371/journal.pone.0130350.

[44] A.M. Hirst, F.M. Frame, N.J. Maitland, D. O'Connell, Low temperature plasma: a novel focal therapy for localized prostate cancer? BioMed Res. Int. 2014 (2014) https://doi.org/10.1155/2014/878319.

[45] D. Hua, D. Cai, M. Ning, L. Yu, Z. Zhang, P. Han, X. Dai, Cold atmospheric plasma selectively induces G0/G1 cell cycle arrest and apoptosis in AR-independent prostate cancer cells, J. Cancer 12 (2021) 5977–5986, https://doi.org/10.7150/jca.54528.

[46] A.M. Hirst, M.S. Simms, V.M. Mann, N.J. Maitland, D. O'Connell, F.M. Frame, Low-temperature plasma treatment induces DNA damage leading to necrotic cell death in primary prostate epithelial cells, Br. J. Cancer 112 (2015) 1536–1545, https://doi.org/10.1038/bjc.2015.113.

[47] Z. He, K. Liu, L. Scally, E. Manaloto, S. Gunes, S.W. Ng, M. Maher, B. Tiwari, H. J. Byrne, P. Bourke, et al., Cold atmospheric plasma stimulates clathrin-dependent endocytosis to repair oxidised membrane and enhance uptake of nanomaterial in glioblastoma multiforme cells, Sci. Rep. 10 (2020) 1–12, https://doi.org/10.1038/s41598-020-63732-y.

[48] G. Daeschlein, S. Scholz, S. Lutze, A. Arnold, S. von Podewils, T. Kiefer, T. Tueting, O. Hardt, H. Haase, O. Grisk, et al., Comparison between cold plasma, electrochemotherapy and combined therapy in a melanoma mouse model, Exp. Dermatol. 22 (2013) 582–586, https://doi.org/10.1111/exd.12201.

[49] O. Estupiñan, L. Santos, A. Rodriguez, L. Fernandez-Nevado, P. Costales, J. Perez-Escuredo, M.A. Hermosilla, P. Oro, V. Rey, J. Tornin, et al., The multikinase inhibitor EC-70124 synergistically increased the antitumor activity of doxorubicin in sarcomas, Int. J. Cancer 145 (2019) 254–266, https://doi.org/10.1002/ijc.32081.

[50] J. Tornin, L. Martinez-Cruzado, L. Santos, A. Rodriguez, L.E. Núñez, P. Oro, M. A. Hermosilla, E. Allonca, M.T. Fernández-García, A. Astudillo, et al., Inhibition of SP1 by the mithramycin analog EC-8042 efficiently targets tumor initiating cells in sarcoma, Oncotarget 7 (2016) 30935–30950, https://doi.org/10.18632/oncotarget.8817.

[51] L.C. Kimlin, G. Casagrande, V.M. Virador, In vitro three-dimensional (3D) models in cancer research: an update, Mol. Carcinog. 52 (2013) 167–182, https://doi.org/10.1002/mc.21844.

[52] A. Alfranca, L. Martinez-Cruzado, J. Tornin, A. Abarrategi, T. Amaral, E. De Alava, P. Menendez, J. Garcia-Castro, R. Rodriguez, Bone microenvironment signals in osteosarcoma development, Cell. Mol. Life Sci. 72 (2015) 3097–3113.

[53] P.D. Ottewell, The role of osteoblasts in bone metastasis, J. Bone Oncol. 5 (2016) 124–127, https://doi.org/10.1016/j.jbo.2016.03.007.

[54] A. Suvannasankha, J.M. Chirgwin, Role of bone-anabolic agents in the treatment of breast cancer bone metastases, Breast Cancer Res. 16 (2014).

[55] L. Gilbert, X. He, P. Farmer, S. Boden, M. Kozlowski, J. Rubin, M.S. Nanes, Inhibition of osteoblast differentiation by tumor necrosis factor-α, Endocrinology 141 (2000) 3956–3964, https://doi.org/10.1210/endo.141.11.7739.

[56] D. Mendoza-Villanueva, L. Zeef, P. Shore, Metastatic breast cancer cells inhibit osteoblast differentiation through the Runx2/CBFβ-dependent expression of the Wnt antagonist, sclerostin, Breast Cancer Res. 13 (2011) R106, https://doi.org/10.1186/bcr3048.